



organized in cooperation with:



4 June – 6 July 2012  
ESSL Research and Training Centre  
Wiener Neustadt, Austria

# ESSL Testbed 2012

## Operations Plan

ESSL Technical Report 2012-01

Final Version

The ESSL Testbed is supported by:



For the 2012 Testbed, ESSL cooperates with the European Centre for Medium-range Weather Forecasts (ECMWF) and the World Meteorological Organization (WMO) - Region VI.

Operations Plan written by:

Pieter Groenemeijer  
Alois M. Holzer  
Kathrin Riemann-Campe

with contributions from:

Kristopher Bedka  
Wayne Feltz  
Caroline Forster  
Hannamari Jaakkola  
Fernando Prates  
Martin Setvák  
Ivan Tsonevsky

European Severe Storms Laboratory – Science and Training  
Bräunlichgasse 6a / 6  
2700 Wiener Neustadt, Austria

Tel: +49 151 59031839  
Tel: +49 8153 281845  
Fax: +49 8153 96599911  
e-mail: [testbed@essl.org](mailto:testbed@essl.org)

Testbed website:

<http://essl.org/testbed>

# Contents

|  |    |
|--|----|
| Contents   | 3  |
| Introduction and goals   | 4  |
| 1.1 Impact of convective storms .....  | 4  |
| 1.2 ESSL Testbed Approach .....  | 4  |
| 1.3 Participants .....   | 5  |
| 1.4 Facilities .....   | 6  |
| 2 Operations   | 7  |
| 2.1 Overview .....   | 7  |
| 2.2 Experimental convective forecasts .....  | 9  |
| 2.3 Forecast verification .....  | 12 |
| 2.4 Evaluation and reporting .....   | 12 |
| 2.5 Expert Lectures .....  | 12 |
| 2.6 Participation schedule .....   | 13 |
| 3 Forecast-supporting products   | 14 |
| 3.1 Standard meteorological data .....   | 15 |
| 3.2 Extreme Forecast Index .....   | 16 |
| 3.3 Cb-TRAM .....  | 17 |
| 3.4 Rad-TRAM .....   | 19 |
| 3.5 Objective Satellite-Based Overshooting Top and Enhanced-V/Cold-Ring Signature Detection .. | 20 |
| 3.6 Objective Satellite-Based Cloud Top Cooling Rate Detection .....                           | 22 |
| 3.7 Vaisala GLD360 .....   | 24 |
| 3.8 COSMO-DE (-EPS) visualizations .....   | 26 |
| 3.9 NowcastMix .....   | 27 |
| 3.10 MSG SEVIRI HRV & IR10.8 BT Sandwich Product .....   | 28 |
| 3.11 European Severe Weather Database, ESWD .....  | 30 |
| Appendix 1: List of on-site participants   | 31 |
| Appendix 2: Expert Lectures  | 32 |
| Appendix 3: References   | 33 |

# Introduction and goals

## 1.1 Impact of convective storms

In Europe, thunderstorms are increasingly being recognized as an important risk to life and property. According to the Munich Re Group, a yearly total damage of about € 5 billion (Munich Re Group, 2006) is inflicted by thunderstorm-related high-impact weather (hail, flash floods, straight-line winds, tornadoes, and lightning) in Europe, comparable in magnitude to that of windstorms. Additionally, such events cause fatalities and injuries as shown in Table 1. Improved forecasts and warnings for severe thunderstorms will result in large societal benefits.

| location                         | country | date           | type of event | killed/injured |
|----------------------------------|---------|----------------|---------------|----------------|
| Hasselt                          | Belgium | 19 August 2011 | downburst     | 4/140          |
| Sosnovo<br>near St. Petersburg   | Russia  | 29 July 2010   | downburst     | 18/ -          |
| Draguignan,<br>Trans-en-Provence | France  | 15 June 2010   | flash flood   | 17/ -          |
| near Messina                     | Italy   | 1 October 2010 | flash flood   | 17/79          |
| Hautmont                         | France  | 3 August 2008  | tornado       | 3/13           |
| Budapest                         | Hungary | 20 August 2006 | downburst     | 1/100          |

**Table 1. Selection of recent thunderstorm-related high-impact weather in Europe**  
(source: European Severe Weather Database, [www.eswd.eu](http://www.eswd.eu))

## 1.2 ESSL Testbed Approach

The ESSL Testbed will assess and improve forecasting and nowcasting techniques of convective high-impact weather by providing institutional human and technical capacity building, accessible to both developed and developing countries in Europe.

Within the Testbed, occurrences of high-impact weather across Europe will be investigated during a yearly test period of 5 weeks in spring, starting in 2012.

The Testbed's concrete aims are...

1. to assess the ability of new diagnostic products based on satellite measurements, numerical weather prediction, radar and standard weather observations to correctly identify (upcoming) severe weather events (e.g. via subjective and objective verification procedures).
2. to obtain feedback from forecasters regarding these products, both with respect to their performance and the operational needs and constraints. This feedback helps the product developers to refine and optimize them, thereby accelerating their successful operational deployment.
3. to familiarize the forecasters of the European National (Hydro-)meteorological Services with the correct use of the new products
4. to enhance the forecasters' overall skills in forecasting of convective high-impact weather, both through remote learning in cooperation with EUMETCAL and "hands on" at the ESSL Training Centre.

The key factor in the Testbed is to ***stimulate interaction between and among developers and forecasters*** which benefits the forecast and warning process at European National Meteorological Services.

The Testbed is loosely modelled after its US counterpart, the Hazardous Weather Testbed Spring Experiment, an annual programme in which several branches of the National Oceanographic and Atmospheric Administration (NOAA) cooperate, including the Storm Prediction Center (SPC) and the National Severe Storms Laboratory (NSSL).

### 1.3 Participants

Testbed participants come from several groups. Since NOAA's Spring Program has proven over the years that interaction between participants with a more scientific background and forecasters is of extremely high value, both groups should be well-represented. Participants therefore include:

- forecasters from Europe's National (Hydro-)Meteorological Institutes
- scientists from these institutes, as well as from international organizations, like EUMETSAT and ECMWF
- scientists or forecasters with a high level of expertise in the forecasting of convective high-impact weather

## 1.4 Facilities



**Fig 1. The ESSL Training Centre in Wiener Neustadt, Austria**

The ESSL Testbed is located in the ESSL Training Center in Wiener Neustadt, a historical imperial city 45 km south of Vienna and 60 km southeast of the Vienna International Airport. The main train station of Wiener Neustadt with frequent trains to Vienna and other Central European Destinations is only 300 m away, thus within walking distance.

The Testbed facilities are housed on the first floor of an Art Deco Style house (Fig. 1) near the town center of Wiener Neustadt. The Testbed and briefing rooms are situated on 150 m<sup>2</sup>, which also include the secretariat and break rooms.

## 2 Operations

### 2.1 Overview

The operations include the following three fundamental components:

1. **forecasting**
2. **verification**
3. **evaluation**

Within the forecasting activities, participants operationally use the experimental forecast products to generate a forecast. After the period for which the forecast was valid has passed, they are verified against observations. Finally, the use of the experimental forecast products is evaluated. Below, these activities are described in more detail.

In addition, there are

- expert lectures (**lecture of the day**)

Within a daily online session, remote participants will receive a briefing of the forecasting, verification and evaluation efforts and are asked to provide feedback and questions. Subsequently, the “lecture of the day” will be transmitted online.

The daily Testbed programme is shown in Table 2, below.

**Daily programme**

| time<br>(local, UTC)                               | activity  | Description   |
|--|---|---|
| 08:30 0630   | Welcome and plan of the day   |   |
| 08:45 0645   | Verification  | Subjective verification of yesterday’s experimental convective forecasts compared to ESWD severe weather reports, satellite and radar data.   |
| 09:15 0715   | Forecast operations   | The participants will be split into two groups, each dealing with a particular forecast period.<br><br>Team A: Day 2 – 5 forecast<br><br>Experimental probabilistic convective forecast for day 2 to 5 using available Testbed products including ECWMF model and high-resolution model data.<br><br>Team B: Day 1 forecast<br><br>Experimental probabilistic convective forecast for the present day using available Testbed products including high-resolution ensembles, and ECWMF model and satellite data. |
| <b>Part of programme with remote participation</b> |   |   |
| 11:00 0900   | Daily briefing  | Online weather briefing, discussion of current weather situation and forecasts and subjective evaluation with remote participants: summarizing new insights, preliminary findings, and topic areas needing further examination.   |
| 11:30 0930   | Lecture of the day  | Expert lecture on forecasting techniques, given by developers of forecast tools or forecasting experts.   |
| around 12:30                                       | ~1030 Lunch break   |   |
| 13:45 1145   | Forecast tool performance evaluation  | Participants jointly fill in a questionnaire on forecast tool performance and add comments to the Testbed Log.  |
| 14:15 1215   | Short-range forecast and nowcast operations or<br><br>Study of past cases, or<br><br>Forecasting training | 1. Experimental short-range forecast and nowcast forecasts of convective initiation and severe weather occurrence. Issuance of experimental warnings, or<br><br>2. Studies of real past forecast situations, or<br><br>3. Severe weather forecasting training by an expert.   |
| 1730 1530  | end   | Formal end time of nowcast operations. Weather permitting, activities may be continued into the evening.  |

**Table 2. The Testbed’s daily programme**

## 2.2 Experimental convective forecasts

On a daily basis, participants will prepare experimental forecasts for severe weather. These forecasts differ in time range, validity time period, domain, and quantities to be forecast. They range from Nowcasts, that have validity time of two hours starting at the moment the forecasts issuance, to Day 5 forecasts, that deal with the weather occurring four days ahead. The forecasts will be issued using a programme with which draw lines are drawn to designate areas in which a particular probability of severe weather or lightning is expected. Table 3 lists all forecasts and areas that may be drawn.

| Type           | Deadlines (UTC)  | Validity (UTC)                            | Predictands   | Domain              |
|----------------|--|---|---|---------------------|
| <b>Nowcast</b> | 1300 (1500 CEST)<br>1400 (1600 CEST)<br>1500 (1700 CEST) | 1300 – 1500<br>1400 – 1600<br>1500 – 1700 | <b>watch</b> with indication of expected severe weather type  | selected sub-domain |
| <b>Day 1</b>   | 0855 (1055 CEST)   | 0900 – 0600 (next day)                    | <b>thunder 15 %</b><br><b>thunder 50 %</b><br>level 1 (> 5% severe)<br>level 2 (> 15% severe)<br>level 3 (> 15 % extreme) | selected sub-domain |
| <b>Day 2</b>   | 0800 (1000 CEST)   | 0600 (next day) –<br>0600 (day + 2)       | <b>thunder 15 %</b><br><b>thunder 50 %</b><br>level 1 (> 5% severe)<br>level 2 (> 15% severe)<br>level 3 (> 15 % extreme) | selected sub-domain |
| <b>Day 3</b>   | 0855 (1055 CEST),<br>on Mondays:<br>1300 (1500 CEST)     | 0600 (day + 2) –<br>0600 (day + 3)        | <b>severe</b>   | Europe              |
| <b>Day 4</b>   |  | 0600 (day + 3) –<br>0600 (day + 4)        | <b>severe</b>   | Europe              |
| <b>Day 5</b>   |  | 0600 (day + 4) –<br>0600 (day + 5)        | <b>severe</b>   | Europe              |

**Table 3. Forecasts at the testbed.**

The forecasts are issued at fixed times and deal with a particular forecast domain. In the case of the Day 3, Day 4, and Day 5 forecasts, the domain is Europe in its entirety, whereas the Nowcasts and Day1 and Day 2 forecasts are issued for a sub-domain that is decided based on the pre-conceived likelihood of severe weather occurring within that sub-domain. The subdomains are drawn in Figure 2.

Many of the predictands of the various forecasts relate to the probabilities of severe weather and extreme weather, which, for the ESSL Testbed are defined as in Table 4.

| Severe weather   | Extremely severe weather   |
|--|--|
| <ul style="list-style-type: none"> <li>• hail 2.0 cm or larger in diameter</li> <li>• wind gusts 25 m/s or higher</li> <li>• any tornado</li> <li>• rainfall causing significant damage</li> </ul> | <ul style="list-style-type: none"> <li>• hail with 5.0 cm diameter or larger</li> <li>• wind gusts 32 m/s or higher</li> <li>• tornado F2 or higher</li> </ul> |
| <p>The quantities to be forecast in the Day 1-5 forecasts are the probabilities that lightning / severe / extreme weather occurs within a radius of 40 km of any given point.</p>                  |  |

**Table 4. ESSL Testbed criteria for severe weather.**

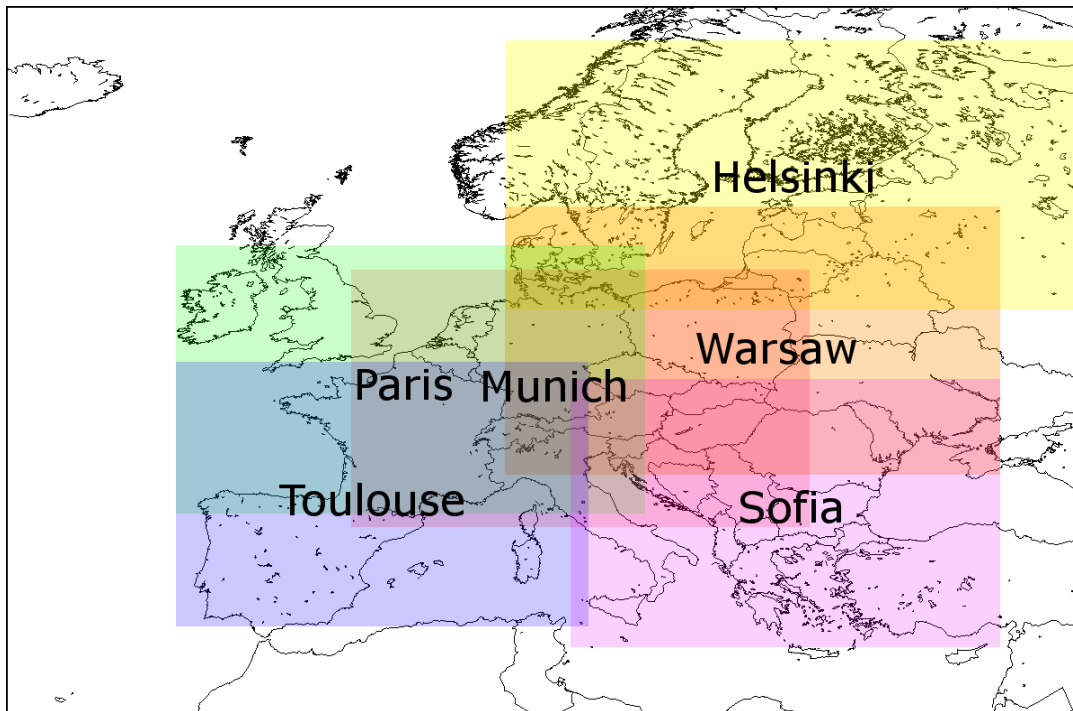


**Fig. 2. The ESSL Testbed domain and the six subdomains for which forecasts are to be made.**

**Nowcasts**

During the afternoon session, starting at 14:15 local time, the groups will work on issuing severe weather warnings for smaller areas within the domain of the day. These are supposed to be warnings for severe weather issued on the order of an hour ahead of time, and with sizes of about 50x50 to 100x100 kilometres.

## Climatology

In case almost no convection is expected across the entire domain, the time slots for forecasting the current weather are used for studying historical cases, or for forecasting workshops organized by expert participants.

Fig 3. shows the coverage of high-impact weather during the Testbed period in previous years. The average number of monthly reports is approximately 1000. Considering that the domain covers the entire European continent (except for Islands and the extreme eastern parts), the weather is usually interesting enough somewhere over Europe.

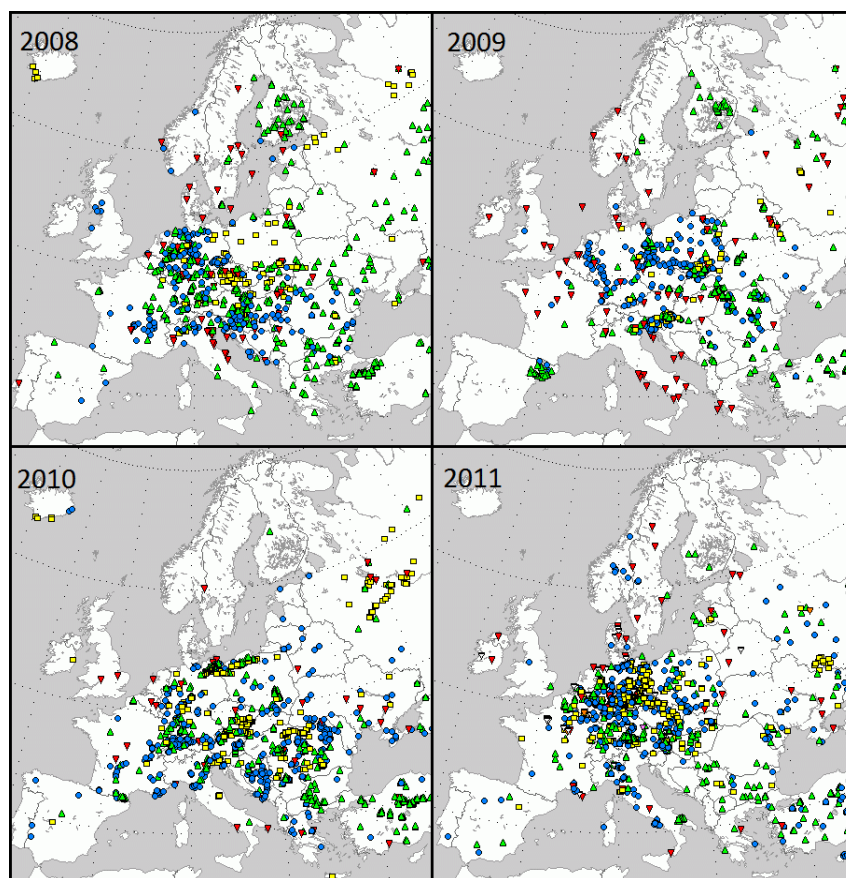


**Fig. 3. High-impact weather coverage during the Testbed period in 2008-2011; yellow rectangles: severe wind gusts, red triangles: tornadoes, blue circles: flash floods, green triangles: large hail (source: ESWD, [www.eswd.eu](http://www.eswd.eu)).**

## 2.3 Forecast verification

During the *verification* slots, the forecasts will be verified subjectively against observed high-impact weather as collected in the European Severe Weather Database (ESSL) and lightning data. For those areas suffering from a low ESWD reporting rate. Areas outside of the lightning detection network will be validated using satellite imagery as a proxy for the occurrence of convection. The outcome of the verification procedure is to establish the magnitude of the discrepancies between forecast and observations and to identify possible causes. These causes may be due to poor guidance by particular data or poor interpretation of the available data.

## 2.4 Evaluation and reporting

In the evaluation sessions, the value of the individual products to the forecast will be assessed. These assessments result from discussions within the group of participants.

Questionnaires, developed for each forecast-supporting product, in collaboration with the partner requesting its testing, are filled in. These questionnaires are listed in chapter 3 and are partly multiple choice, and partly open questions. With each multiple-choice question, it is requested that a motivation is documented. The results of the questionnaires will be added to the Testbed log.

After the end of Testbed operations, the *ESSL Testbed* staff will write a concise report for each Experimental Forecast Product that has been tested, based on the information collected in the *Testbed Log*. These individual reports will be delivered to the ordering party who may decide at their own discretion on the level of dissemination of the report.

Additionally, an overall Testbed report will be produced that will be published as an ESSL Scientific Report. It will be available for download from the ESSL website. The level of detail of the contents regarding particular products will be coordinated with the respective partner.

## 2.5 Expert Lectures

Lectures are presentations 45 minutes in length with 15 minutes time for discussion, that will be disseminated online with support from EUMETCAL following the *Daily Briefing*, starting approximately at 0930 UTC (1130 local time). The lecturers include experts on forecasting, modelling, remote-sensing or other relevant topics. These will include scientists from European weather services and overseas, and from international organizations like EUMETSAT and ECMWF as well as forecasters with a great expertise in the forecasting of convective high-impact weather. A list of speakers is available in Appendix 2.

## 2.6 Participation schedule

### Testbed Groups

Participants to the Testbed, forecasters and scientists/developers, will be assigned to each of five groups. These groups will have sizes of approximately 10-12 persons, not including Testbed staff. In practice, and taking into consideration other obligations of the participants, the groups will be filled starting from group 1 through group 5.

### On-site and remote participation

It is recommended that participants first participate one week remotely, followed by a week on site at the ESSL Training Centre in Wiener Neustadt (see Table). The online participation involves connecting to the online session via the Centra web conferencing software supported by EUMETCAL as well as participating in the Daily Briefing, and attending the *Lecture of the day*. These activities take place from 0900 UTC to 1030 UTC, possibly a bit later, and will effectively cost a remote participant about two hours a day. Participants of the first Testbed week will not have the possibility of prior remote participation, but are welcome to attend remotely later.

### 3 Forecast-supporting products

A wide range of tools that support the forecaster in early operational or pre-operational stage (Forecast-Supporting Products) can be tested at the ESSL Testbed. These FSP's can be of very different nature. For example, new versions or configurations of numerical weather prediction models, new techniques to extract information from satellite, radar and other remote sensing data. This includes new visualizations and ways to combine different types of meteorological data relevant to the prediction of high-impact weather. FSP's are listed in Table 2, and described in the sections that follow.

| forecast-supporting product                                   | developer                     | Description  |
|---|-------------------------------|--|
| Extreme Forecast Index  | ECMWF                         | Index allowing identification of forecast extremes by comparing the EPS forecast distribution with the model climate |
| Cb-TRAM and Rad-TRAM  | German Aerospace Center (DLR) | Fully automated tracking and nowcasting algorithms based on satellite and radar data                                 |
| Overshooting Top and Enhanced-V/Cold-Ring Signature Detection | NOAA GOES-R                   | Objective Satellite-Based Overshooting Top and Enhanced-V/Cold-Ring Signature Detection                              |
| Cloud Top Cooling Rate Detection                              | U. Wisconsin / NOAA GOES-R    | Objective Satellite-Based Cloud Top Cooling Rate Detection   |
| GLD360  | VAISALA                       | Global lightning detection network   |
| COSMO-DE-EPS visualizations                                   | DWD / ESSL                    | Visualizations of high-resolution convection permitting ensemble data  |
| NowCastMIX  | DWD                           | Grid-based system combining nowcast data from multiple sources using fuzzy logic                                     |
| Satellite sandwich image products                             | CHMI                          | Blended MSG SEVIRI HRV and colour-enhanced IR10.8 brightness temperature product                                     |
| ESWD  | ESSL                          | European Severe Weather Database in Nowcast mode, providing observations of severe weather in near real-time.        |

*Table 2. Forecast-supporting products.*

### 3.1 Standard meteorological data

In addition to the experimental products described in the following sections, the following “standard” meteorological data will be available, through the Testbed intranet web site.

#### NWP

- ECWMF IFS data is provided by ZAMG, and additionally available through the website of ecmwf.
- ECMWF Ensemble Prediction System, Extreme Forecast Index (source: ECMWF, is part of the testing programme), available both through ZAMG and, with more features, through the website of ecmwf.
- COSMO-EU (source: DWD)
- COSMO-DE (source: DWD; is part of the testing programme)
- COSMO-DE-EPS (source: DWD; is part of the testing programme)
- ALARO (source: ZAMG)
- GFS (source: NCEP)

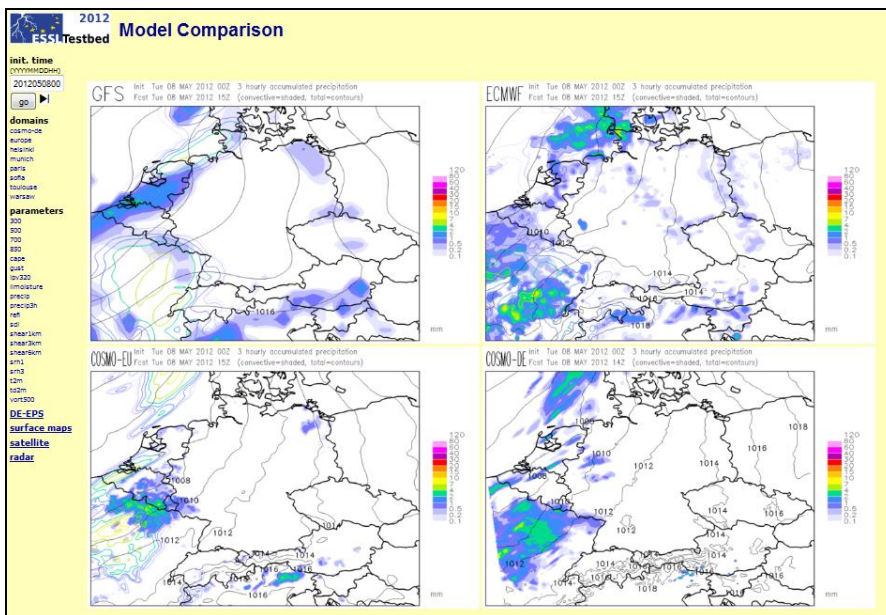


Figure. ESSL Testbed NWP model comparison webpage.

#### Satellite

From Meteosat 9 (available every 15 minutes):

- E-View, High Resolution Visible, IR-10.8, IR-10.8 (color enhanced), Airmass-RGB, Severe Storm RGB, WV-7.3

From Meteosat 8 RapidScan service (available every 5 minutes):

- E-View, High Resolution Visible, IR-10.8, IR-10.8 (color enhanced), Severe Storm RGB

From these products, two “Sandwich Products” (see section 3.11) are computed by ESSL, both from Meteosat 9 and from MeteoSat8 RapidScan data.

### **Radar imagery**

- The European radar composite OPERA will become available during the first Testbed week

### **Surface observations of Europe**

- Surface observations are delivered to ESSL by ZAMG and are displayed on printable maps and as overlays on satellite imagery.

### **Radiosonde data**

- Radiosonde data are available on the internet through the University of Wyoming and the University of Oklahoma

### **Severe weather observations**

- Severe weather observations are available from the European Severe Weather Database (see Section 3.12).

### **Lightning data**

- Two sources of lightning data are available. Firstly the GLD360 product by Vaisala which is part of the testing programme (Section 3.7), and, secondly, data from the ground-based EUCLID network which can be accessed through a web interface.

## **3.2 Extreme Forecast Index**

Fernando Prates, Ivan Tsonevsky (ECMWF)

The Extreme Forecast Index (EFI) has been developed at ECWFMF to alert forecasters to anomalous or extreme weather events by comparing the Ensemble Prediction System (EPS) forecast with the model climate. The advantage of using the EFI is that it is an integral measure of the difference between the EPS forecast distribution and the model climate distribution that contains all the information regarding variability of a parameter in location and time. Therefore, the users can recognise the abnormality of the weather situation without defining different space- and time-dependent thresholds. The EFI takes values from -1 to +1. If all the EPS members forecast values above the climate maximum,  $EFI = +1$ ; if they all forecast values below the climate minimum,  $EFI = -1$ . If the EPS probability distribution is no different from the model climate distribution then  $EFI = 0$ . Experience suggests that EFI values of 0.5 - 0.8 (irrespective of sign) can be generally regarded as signifying that “unusual” weather is likely and values above 0.8 as

usually signifying that “very unusual” or extreme weather is likely. Although higher EFI values indicate that an extreme event is more likely, the values do not represent probabilities, as such.

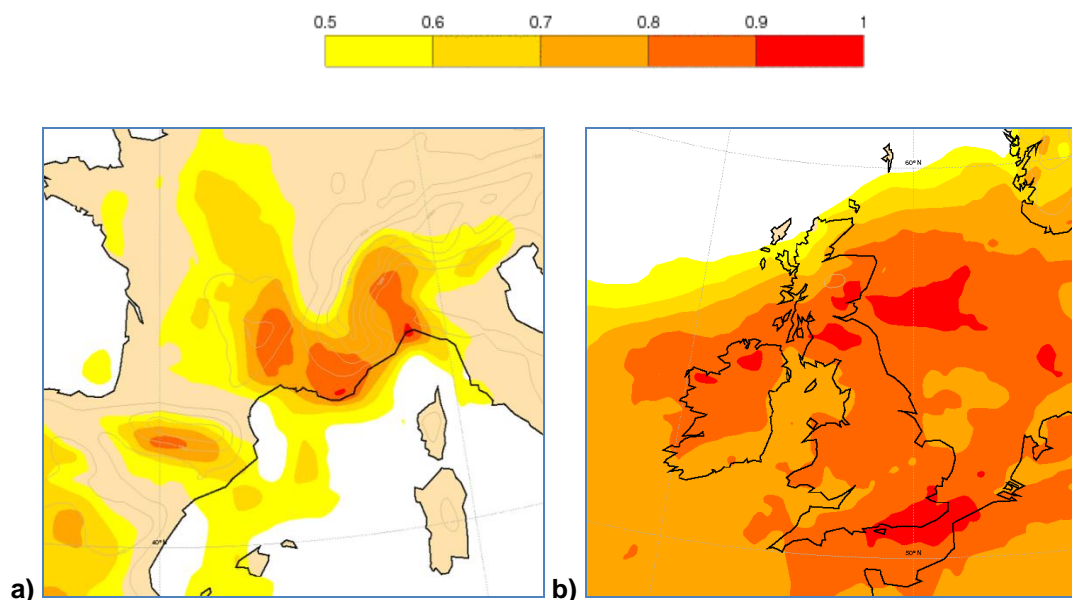


**Figure: Extreme Forecast Index for a) 5-day accumulated precipitation during the floods in Italy and France from 2<sup>nd</sup> to 6<sup>th</sup> November 2011; forecast from 1<sup>st</sup> November 00UTC, T+24-144h and b) 24-h maximum wind gusts during the wind storm over the UK on 3<sup>rd</sup> January 2012; forecast from 1<sup>st</sup> January 00UTC, T+48-72h.**

The EFI is computed out to five days ahead for 10 m wind (daily mean), 10 m wind gusts (daily maximum), 2 m temperature (daily mean), precipitation (daily accumulations up to day 5 and for the intervals 1-5, 2-6 and 1-10 days).

In the near future the EFI will be computed for additional parameters, including 2 m maximum and minimum temperatures and snowfall. The forecast time ranges will also be extended up to seven days ahead. For 2 m mean temperature, 10 m wind speed and precipitation longer time ranges will be available up to day 15. A new Shift Of Tails (SOT) index will complement the EFI providing information about the magnitude of the potential extreme event.

### 3.3 Cb-TRAM

Caroline Forster (German Aerospace Center DLR)

Cb-TRAM (Zinner et al., 2008; Zinner and Betz, 2009) stands for Cumulonimbus Tracking and Monitoring and is a fully automated tracking and nowcasting algorithm. Intense convective cells are detected tracked and discriminated with respect to onset, rapid development, and mature phase. The detection is based on Meteosat SEVIRI (Spinning Enhanced Visible and Infra-Red Imager) data from the broad band high resolution visible, infra-red 6.2 mm (water vapour), infra-red 12.0  $\mu\text{m}$  and infra-red 10.8 mm channels.

The tracking is based on geographical overlap between current detections and first guess patterns of cells predicted from preceding time steps. The first guess patterns as well as short range forecast extrapolations are obtained with the aid of a new image matching algorithm providing complete fields of approximate differential cloud motion. Based on these motion vector fields interpolation and extrapolation of satellite data are obtained which allow to generate synthetic intermediate data fields between two known fields as well as nowcasts of motion and development of detected areas.

Two different Cb-TRAM products are provided to the ESSL Testbed.

- Cb-TRAM normal scan:

Here, Cb-TRAM is based on METEOSAT-9 data which are available every 15th minute.

- Cb-TRAM rapid scan:

Here, Cb-TRAM is based on METEOSAT-8 rapid scan data which are available every 5th minute.

During the ESSL Testbed in 2012, Cb-TRAM rapid scan is provided for three different geographical areas: an overview of Germany and neighbouring countries (Cb-TRAM rapid scan overview), a view of the Terminal Maneuvring Area (TMA) Munich (MUC) (Cb-TRAM rapid scan TMA\_MUC), and a view around Wiener Neustadt (Cb-TRAM rapid scan Wiener Neustadt).

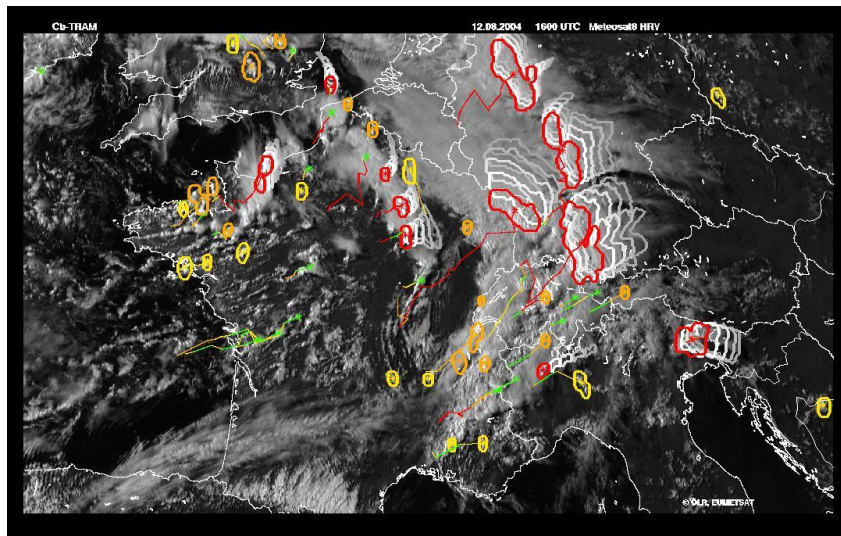


**Figure: Example of the Cb-TRAM display. Yellow, orange, and red contours represent on-set, rapid development and mature thunderstorms. The 15, 30, 45, and 60 minutes nowcasts are indicated as grey contours. The coloured lines are the tracks of the cell centres.**

### 3.4 Rad-TRAM

Caroline Forster (German Aerospace Center DLR)

Rad-TRAM (Kober and Tafferner, 2009) stands for Radar Tracking and Monitoring and is a fully automated tracking, monitoring, and nowcasting algorithm. It uses reflectivities of a radar composite from the German Weather Service (DWD) to detect and nowcast (= short-range forecast up to 1 hour) precipitation cells  $\geq 37\text{dBZ}$ , i.e. areas with heavy precipitation or hail (see image below). The tracking and nowcasting is based on the same image matching technique as in Cb-TRAM.

Three different products are provided:

- Rad-TRAM RX

Here, Rad-TRAM is based on the DWD RX radar composite for Germany which is updated every 5th minute and has a spatial resolution of 1km x 1km.

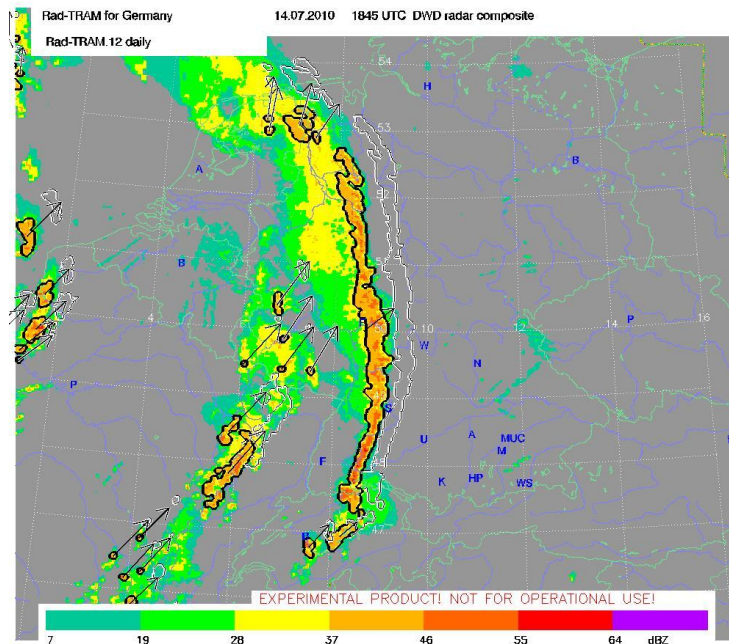
- Rad-TRAM Euradcom

Here, Rad-TRAM is based on the DWD EURADCOM radar composite for FABEC (Functional Airspace Block Europe Central) which is updated every 5th minute and has a spatial resolution of 1km x 1km.

- Rad-TRAM PM

Here, Rad-TRAM is based on the DWD European radar composite (PM product) which is updated every 15th minute and has a spatial resolution of 2km x 2km.

The Rad-TRAM RX product is provided for three different geographical areas: an overview of Germany and neighbouring countries (Rad-TRAM RX overview), a view of the Terminal Maneuvring Area (TMA) Munich (MUC) (Rad-TRAM RX TMA\_MUC), and a detailed view around Munich (MUC) Airport (Rad-TRAM RX MUC Airport).



**Figur:** Example of the Rad-TRAM display. The black contours represent heavy precipitation cells  $\geq 37$ dBZ. The thin white contours are the 60 minutes nowcasts. The arrows indicate the moving direction of the cells.

### 3.5 Objective Satellite-Based Overshooting Top and Enhanced-V/Cold-Ring Signature Detection

Kristopher Bedka, Science Systems and Applications, Inc. @ the NASA Langley Research Center (supported by the NOAA GOES-R Visiting Scientist Program)

Overshooting tops (OTs) are produced by deep convective updraft cores of sufficient strength to rise above the storms’ general equilibrium level near the tropopause region and penetrate into the lower stratosphere. OTs appear in  $\sim 11 \mu\text{m}$  longwave IR window imagery as a small cluster ( $< 15 \text{ km}$  diameter) of very cold pixels relative to the surrounding cirrus anvil cloud. An OT with a significant vertical protrusion above the surrounding cirrus anvil cloud can act as an obstruction to the jet stream wind flow. OTs often inject a significant amount of water vapor into the lower stratosphere which can condense to form a cirrus plume which resides at a height above the primary cirrus anvil cloud. A region of anomalously warm IR brightness temperatures (BTs) is often found downstream of the OT region in conjunction with the above-anvil cirrus plume which radiates at the stratosphere temperature that is warmer than the primary anvil. These two processes combine to produce patterns in IR satellite imagery known as the “cold-ring” or the “enhanced-V signature” (see Figure below). Cold-ring signatures are often found in regions of weaker jet stream winds than enhanced-V signatures, though a storm top pattern can evolve between a V- and cold-ring signature throughout the storm lifetime (Setvak et al. 2010). The combination of the cold OT

signature and downstream warm region within the enhanced-V or cold-ring will be referred to here as an anvil thermal couplet (ATC).

Thunderstorms with OTs frequently produce hazardous weather at the Earth's surface such as heavy rainfall, damaging winds, large hail, and tornadoes. Maximum radar reflectivity and precipitation echo top height is found at or near the time of OT detections (Dworak et al. 2012). Turbulence and lightning are often concentrated near the OT region, indicating that OTs represent significant hazards to ground-based and in-flight aviation operations. Thunderstorms with a strong ATC signature (i.e. OT minus warm region BT diff > 8 K) have been shown to be especially severe (Brunner et al. 2007). Dworak et al. (2012) and McCann (1983) show that the OT and enhanced-V signatures can appear 30 minutes before the onset of severe weather on the ground, providing a forecaster with crucial situational awareness and possibly additional warning lead time.

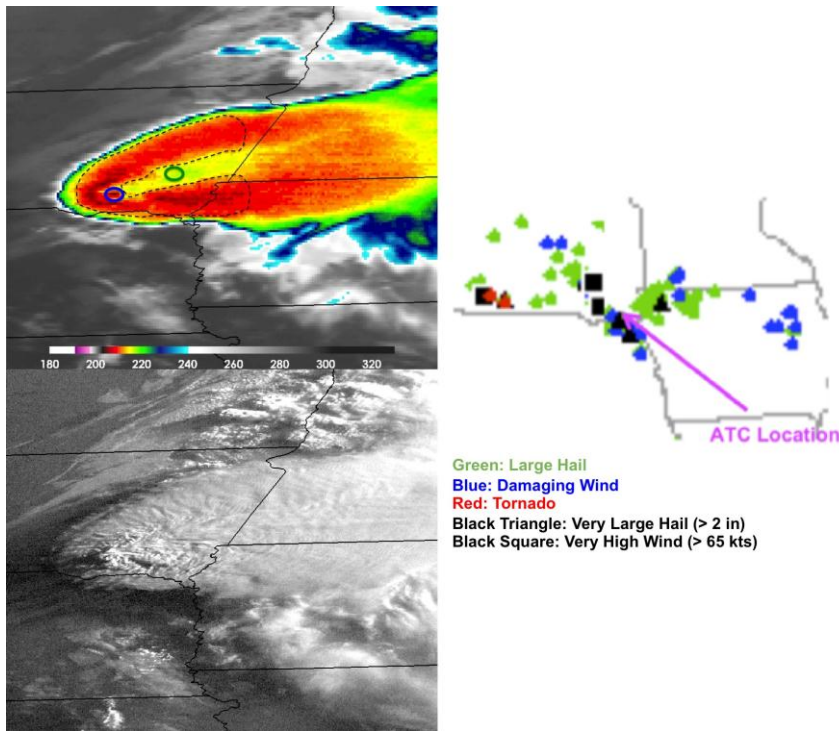


**Figure. (upper-left)** An enhanced-V producing storm over the U.S. Northern Plains in GOES-12 IR window channel imagery on 9 July 2009. The enhanced-V signature is outlined with a dashed line, the objective OT detection is shown with a blue circle, and the downstream warm region detection is shown with a green circle. **(lower-left)** GOES-12 Visible channel image for the same scene. **(right)** Severe weather reports associated with this storm. The location of the storm in the GOES image is shown, indicating that the storm was producing significant severe weather at the time of OT and enhanced-V detection.

Objective satellite-based OT and ATC detection algorithms have been developed for the GOES-R Aviation Algorithm Working Group (Bedka et al. 2010; Bedka et al. 2011). As the OT and ATC are often small in size and short-lived, the algorithms perform optimally with  $\leq 2$  km spatial and  $\leq 5$  min temporal resolution imagery but they can be applied to current 15 min 3 km MSG SEVIRI and 4 km GOES

imagery. The OT detection component uses a combination of IR window channel brightness temperatures (BTs), a NWP model tropopause temperature forecast, and OT size and BT criteria defined through analysis of OT producing storms in GOES, MODIS, and AVHRR imagery. The enhanced-V/cold-ring ATC detection algorithm requires detection of the OT. A set of spatial IR BT and BT gradient checks are performed throughout the anvil cloud surrounding the OT to identify a significant downstream warm region that composes the ATC. Validation studies indicate an OT detection POD and FAR of ~30-50% and 6-20% for current geostationary image inputs, respectively, depending on the dataset used to define an OT event. ATC detection has not been validated for current geostationary imagery.

Two products will be provided via a webpage for evaluation within the 2012 ESSL Testbed: 1) an OT detection mask, and 2) an ATC (i.e. enhanced-V or cold-ring) detection mask.

### **3.6 Objective Satellite-Based Cloud Top Cooling Rate Detection**

Justin Sieglaff and Wayne Feltz (University of Wisconsin – Madison, Cooperative Institute for Meteorological Satellite Studies)

Short-term (0–1 h) convective storm nowcasting remains a problem for operational weather forecasters. Numerical weather prediction models, traditional meteorological observations, and radar are useful for short-term convective weather forecasting, but all have shortcomings. Geostationary imagers, while having their own shortcomings, are valuable assets for addressing the convective initiation nowcast problem. Geostationary satellite data can be used to detect new convective clouds and monitor their initial growth before precipitation is detected by weather radar. The University of Wisconsin (UW) – Cloud Top Cooling rate (CTC) algorithm is an experimental satellite based product used to diagnose infrared window channel brightness temperature cloud top cooling rate and to nowcast convective initiation (Sieglaff et al, 2011). The UW-CTC algorithm uses geostationary imager data to identify immature convective clouds that are growing vertically and cooling in infrared satellite imagery. Additionally, cloud phase information is utilized to deduce whether the cooling clouds are immature water clouds, mixed phase clouds or ice-topped (glaciating) clouds. The mean POD and FAR are 56.3% and 25.5%, respectively, for regions within a severe storm risk area defined by the NOAA Storm Prediction Center.

While instantaneous UW-CTC rate can be used to highlight vertical cloud growth, the cloud's maximum UW-CTC rate during the convective initiation phase is very useful for predicting future radar echo intensification (Hartung et al. 2012). UW-CTC rates have proven to be most skillful for detecting convective clouds that achieved intense radar signatures [e.g. POD of 65.0% for cloud-objects that developed a 60+ dBZ reflectivity echo at the -10°C isotherm, 64.0% for those that developed a VIL of 35+ kg m<sup>-3</sup>, and 71.0% for storms that attained a severe radar estimated hail size (MESH) of 1.00"+]. Results suggest that convective clouds with the strongest UW-CTC rates are more likely to achieve significant near-term (0-60 minutes) radar signatures in such fields as composite reflectivity, VIL, MESH, and high 18+ dBZ echo tops compared to weaker convective growth clouds. The UW-CTC product will be provided via a webpage for evaluation within the 2012 ESSL Testbed

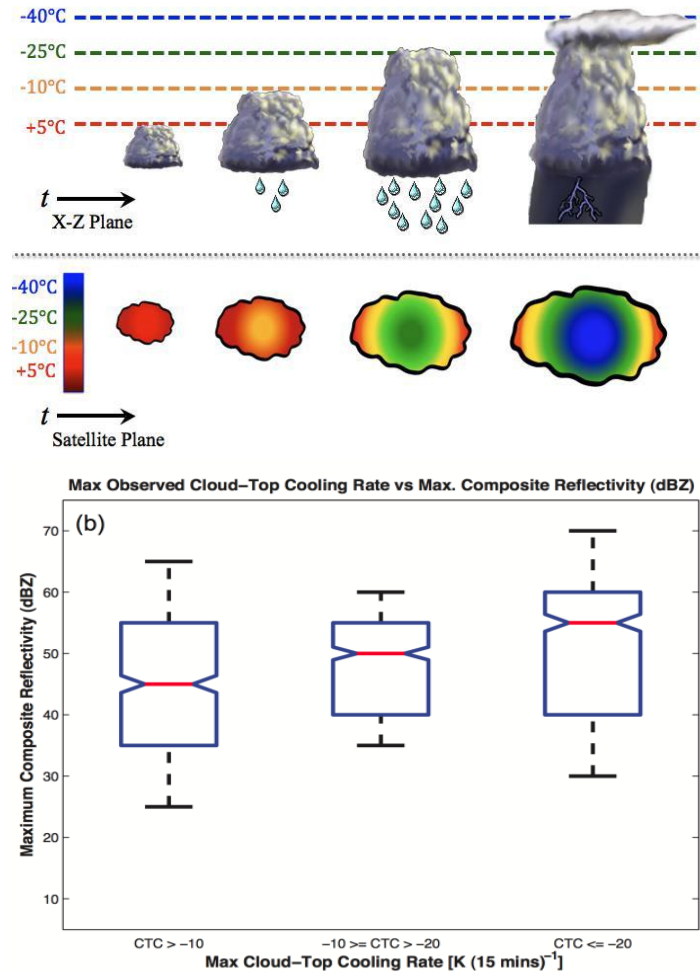


Figure: Conceptual model of a developing cumulonimbus cloud illustrating how cloud-top temperature decreases with increased vertical growth and maturation over time in the X-Z plane (top) and as observed in the IR brightness temperature field from a geostationary satellite (middle). (bottom) Comparison of maximum UW cloud-top cooling rates to maximum composite reflectivity (dBZ) for clouds that had both a UW-CTC rate and composite reflectivity at some point in their lifetime. UW-CTC rates for cloud-objects are binned by intensity [K/15 min] with weak, moderate, and strong convective growth defined as UW-CTC > -10, -10 ≥ UW-CTC > -20, and UW-CTC ≤ -20, respectively. For each boxplot, the median (red line), 25<sup>th</sup> and 75<sup>th</sup> percentiles (lower and upper bounds of blue box), and one standard deviation (whiskers) are shown. The medians of different intensity bins are significantly different at the 5% significance level if the widths of the notches centered on the medians do not overlap.

### 3.7 Vaisala GLD360

Hannamari Jaakkola (VAISALA)

In 2009, Vaisala launched the Global Lightning Dataset GLD360. GLD360 data is produced by a Vaisala owned and operated lightning detection network that provides uniform, high quality lightning information across the globe. Data delivered includes CG stroke and cloud lightning information – and it can be delivered to the customer in real time.

Patented sensor algorithms and extreme sensitivity give GLD360 sensors the ability to detect lightning at distances up to 9,000 km. Each GLD360 sensor provides both direction and time-of-arrival information. Scientific studies have shown that lightning networks using a combination of direction and time-of-arrival sensor information provide significant detection efficiency and redundancy improvements over lightning networks using time-of-arrival sensor information alone. Through its GLD360 offering Vaisala provides the highest quality global lightning data in the market:

- Location Accuracy (LA): The median cloud-to-ground lightning stroke location accuracy 2-5 km
- Detection Efficiency (DE): 70% for cloud-to-ground flashes and >5% for cloud flashes with near uniform coverage around the globe (ref. the DE map in the Figure 1 below).
- Polarity & Peak Amplitude (kA): Unique to the GLD360 is the ability to provide polarity & peak amplitude (kA), which is typically the reserve of precision networks. The GLD360 polarity classification is greater than 90% and peak current estimates are accurate to within 25 % of the peak current value.

To ensure GLD360 provides the high level of network performance described above, validation studies have been performed in North America, Europe, and are now ongoing in South America. The results of these studies show that GLD360 has a CG flash detection efficiency of 70% or greater and a median CG stroke location accuracy of 2-5 km in all three regions.

Long-range severe weather detection has traditionally been limited by data gaps, leading to situations where people have late or no warnings. GLD360 is the only severe weather data set that has no data gaps and provides a nearly uniform, global coverage. GLD360 routinely detects over 1.5 million lightning events across the world each day.

As your global window, the GLD360 provides immediate access to a world-wide lightning dataset, anywhere around the globe. Vaisala thus has a unique offering that supports:

- Ability to detect and characterize lightning in areas of the world where meteorological observations may be partially lacking or absent.

- Lightning as a radar proxy or radar complement where weather radar information is limited or nonexistent.
- The ability to extend the range of lightning being assimilated into weather models and enhance the foresight of advancing weather systems.
- Quality lightning warnings on a truly global scale.

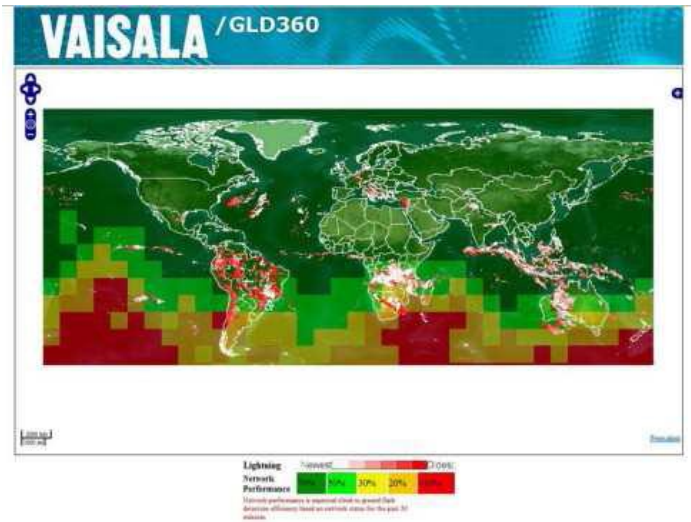


Figure: The global detection efficiency map for GLD360.

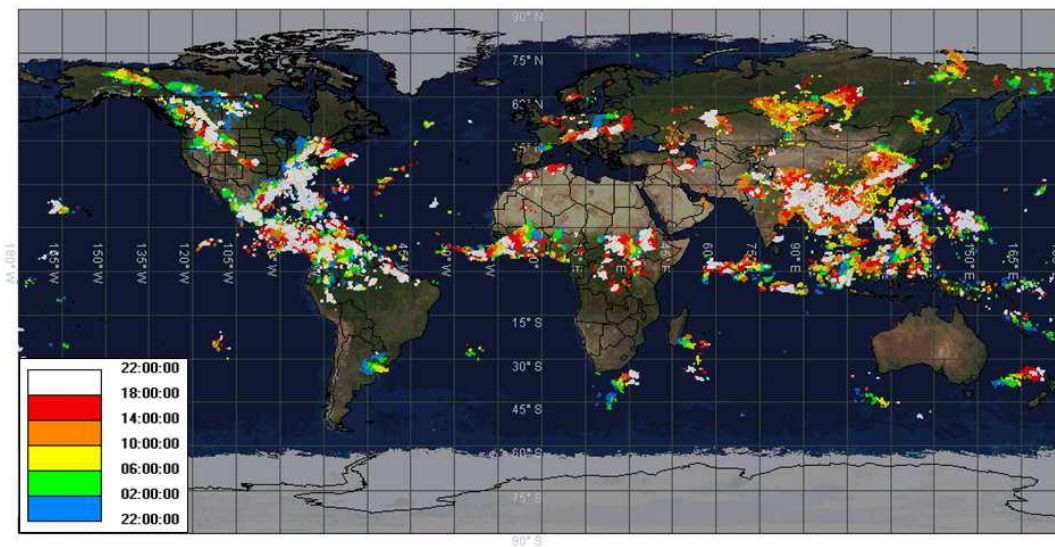


Figure: Global image showing more than two million lightning events reported by GLD360 on 22-23 June 2011. Colors show age of lightning events in 4-hour intervals starting on 22 June at 22:00 and ending on 23 June at 22:00.

### 3.8 COSMO-DE (-EPS) visualizations

Dirk Heizenreder (DWD), Marcus Paulat (DWD), Pieter Groenemeijer (ESSL)

COSMO-DE-EPS is an ensemble of the German Weather Service’s high-resolution, convection permitting model COSMO-DE (COntortium for Small-scale MOdelling - DEutschland). Different initial and boundary conditions of the ensemble members are obtained from four different COSMO runs at 7 km which are in turn driven by different global NWP models (ECMWF IFS, DWD GME, NCEP GFS and UKMO UM) and varying parameters during the assimilation phase. Additionally, the ensemble members use varying model physics parameters.

Visualization of large volumes of ensemble data is a challenge. For example, in plotting the average and standard deviation of forecast quantities much information is lost. For a field like radar reflectivity such a display would not make much sense. At the Testbed, the following visualizations of the following fields will be evaluated:

| Field   | Visualizations   |
|---|--|
| Reflectivity                                    | 1. maximum value of any ensemble member<br>2. coloured areas where any ensemble member exceeds threshold of 40 dBZ                       |
| 10 m wind gust                                  | 1. maximum value of any ensemble member<br>2. coloured areas where any ensemble ensemble member exceeds threshold of 25 m/s              |
| Supercell Detection Index (Wicker et al., 2005) | maximum value of any ensemble member<br>coloured areas where any ensemble member exceeds threshold of 0.001                              |
| 3 hourly accumulated precipitation              | maximum value of any ensemble member<br>coloured areas where any ensemble member exceeds threshold of 20 mm (contours) or 44 mm (shaded) |

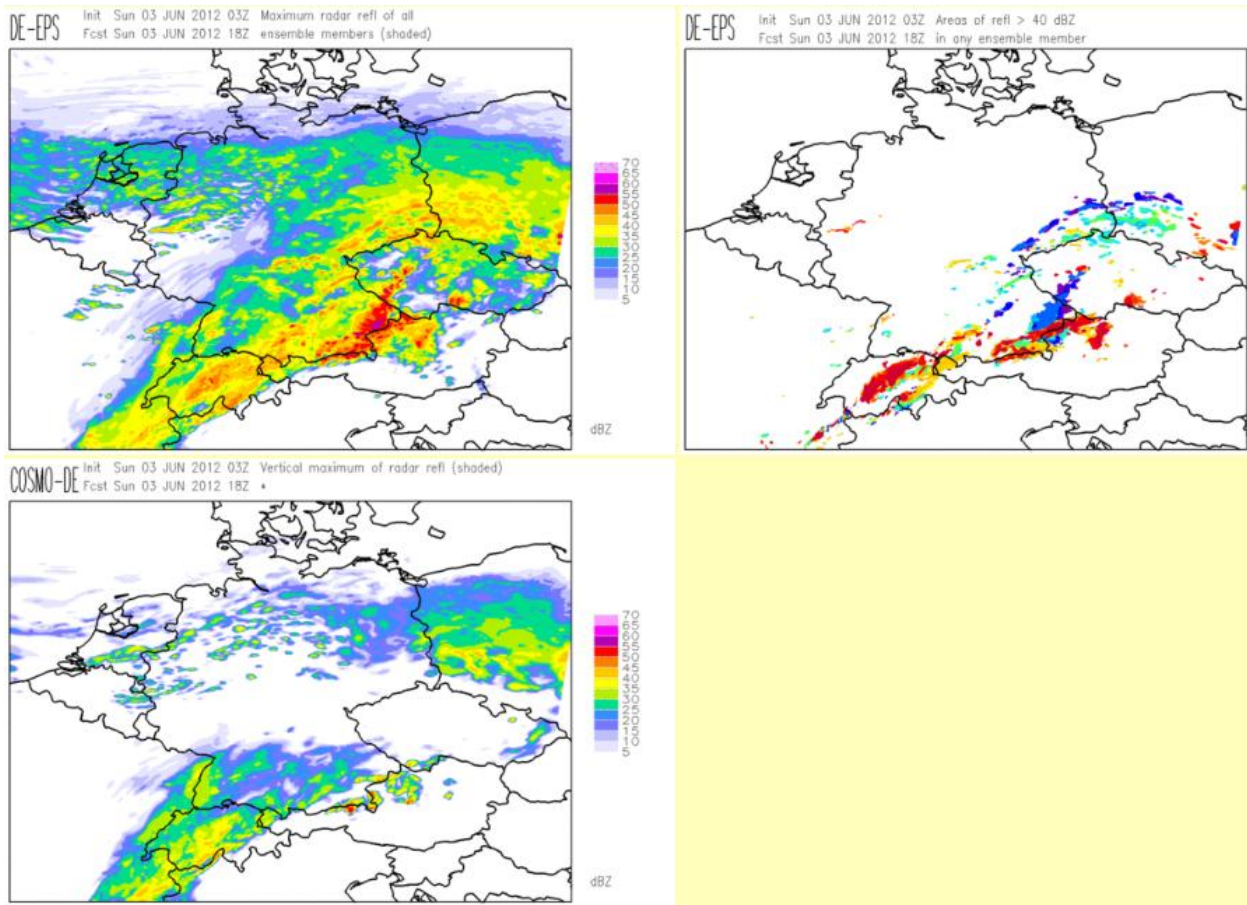


**Figure. Top left: Maximum of any member display of COSMO-DE-EPS, top right: Members exceeding 40 dBZ threshold display, bottom: deterministic COSMO-DE run for comparison.**

### 3.9 NowcastMix

Paul James (DWD)

The GermanWeather Service's AutoWARN system integrates various meteorological data and products in a warning decision support process, generating real-time warning proposals for assessment and possible modification by the duty forecasters. These warnings finally issued by the forecaster are then exported to a system generating textual and graphical warning products for dissemination to customers. On very short, nowcasting timescales, several systems are continuously monitored. These include the radar-based storm-cell identification and tracking methods, KONRAD and CellMOS; 3D radar volume scans yielding vertically integrated liquid water (VIL) composites; precise lightning strike locations; the precipitation prediction system, RadVOR-OP as well as synoptic reports and the latest high resolution numerical analysis and forecast data. These systems provide a huge body of valuable data on rapidly developing mesoscale weather events. However, without some form of pre-processing, the forecasters could become overwhelmed with information, especially during major, widespread summer convective outbreaks. NowCastMIX thus processes all available nowcast data together in an integrated grid-based

analysis, providing a generic, optimal warning solution with a 5-minute update cycle, combining inputs using a fuzzy logic approach. The method includes optimized estimates for the storm cell motion vectors by combining raw cell tracking inputs from the KONRAD and CellMOS systems with vector fields derived from comparing consecutive radar images. Finally, the resulting gridded warning fields are spatially filtered to provide regionally-optimized warning levels for differing thunderstorm severities which can be managed adequately by the duty forecasters. NowCastMIX thus delivers an ongoing real-time synthesis of the various nowcasting and forecast model system inputs to provide consolidated sets of most-probable short-term forecasts.

### **3.10 MSG SEVIRI HRV & IR10.8 BT Sandwich Product**

Martin Setvák (CHMI)

The origins of the sandwich product are closely related to studies of the tops of convective storms. When studying or monitoring certain storm-top features in satellite imagery, it is essential to know their spatial arrangement in various spectral bands or advanced products based on these bands. The most typical example is the comparison of storm-top appearance in a visible band, available at high spatial resolution, with the IR-window brightness temperature (BT) field – e.g. when studying characteristics of the overshooting tops, various BT features (such as cold-U/V or cold ring phenomena), above-anvil plumes, etc. One possibility is comparing the images “side-by-side”, or alternatively fast toggling of the images in various bands forward and backward (usable only on a computer, not in a printed form).

A more efficient and visually appealing option is blending (“sandwiching”) the images together, using one of the blending functions available in some of the graphics editors, such as Adobe Photoshop, GIMP, or ImageMagick. The blended product (“sandwich”) consists of two layers: the base layer, which is usually one of the visible or near-IR bands at the best pixel resolution possible, and the upper layer, containing a field such as the colour-enhanced IR-window image remapped to the same map projection and pixel resolution as the visible band.

The primary advantage of sandwich products is that they merge the features of the two input images into one single image, thus enabling one to observe the characteristics of both images simultaneously in one single product. In the case of the visible – IR-window sandwich combination (VIS/IR-BT), the visible band brings to the final image the cloud-top “morphology” (shadows and textures), while the colour-enhanced IR-window band adds the BT information. Such images often gain almost a 3D appearance, which is absent if the source input images are compared side-by-side. Finally, it is much easier to follow the evolution of convective storms in one single sandwich product, rather than in two windows, showing the input bands separately. This makes the sandwich products very attractive for operational applications.

When preparing the sandwich product images for case studies or publications, it is possible to further increase the quality of the final image by interactive tuning of the product by manually adjusting the options of the blending function. This applies namely when working with stand-alone data sets from

imagers aboard polar orbiters, such as AVHRR, MODIS or VIIRS; one example of such interactively tuned sandwich products at high resolution is shown in Fig. 2, several other examples will be shown in the presentation. However, when processing a series of images from geostationary satellites, and especially for operational applications, the sandwich product has to be generated automatically. For these purposes it is possible to use e.g. the ImageMagick software.

Within the ESSL Testbed 2012, the participants will have an opportunity to evaluate the MSG sandwich product based on HRV and colour-enhanced IR10.8 BT input images, comparing the blended sandwich product with the stand-alone input (source) images. Despite the fact that the sandwich product is not a forecast product, it should enhance the efficiency of convective storms monitoring, namely by easier detection of various severity-related cloud-top features, such as overshooting tops, cold-U/V (enhanced V) and cold ring features. An example of MSG-based sandwich product is at the image below.

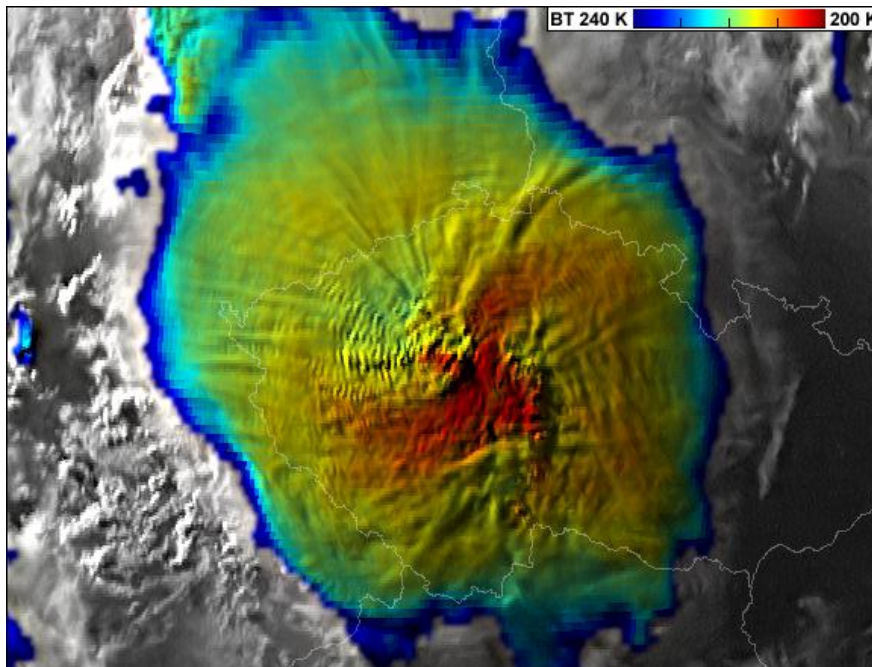


**Figure: Example of a sandwich product based on the MSG HRV and colour-enhanced IR10.8 BT images.**

### 3.11 European Severe Weather Database, ESWD

Pieter Groenemeijer, Thilo Kühne, Alois Holzer (ESSL)

The ESWD (Groenemeijer et al, 2004, 2009; Dotzek et al, 2009) is a dataset of severe weather reports managed by ESSL. The dataset is fed by observations from cooperating National (Hydro-)Meteorological Services, networks of voluntary observers, the general public and by ESSL itself. The following categories of severe weather are included in the ESWD at this time:

- straight-line wind gusts ( $v > 25 \text{ m s}^{-1}$ )
- tornadoes
- large hail (diameter  $> 2 \text{ cm}$ ; or layer  $> 2 \text{ cm}$ )
- heavy precipitation
- funnel clouds
- gustnadoes
- lesser whirlwinds
- damaging lightning strikes
- and the winter weather hazards: heavy snowfalls/snowstorms, avalanches and ice accumulations.

The ESWD database can be run in a *Nowcast mode* that features a map showing the reports in real-time as they are reported by its various sources. At the Testbed, the ESWD's usefulness for both nowcasting and forecast verification purposes will be evaluated.

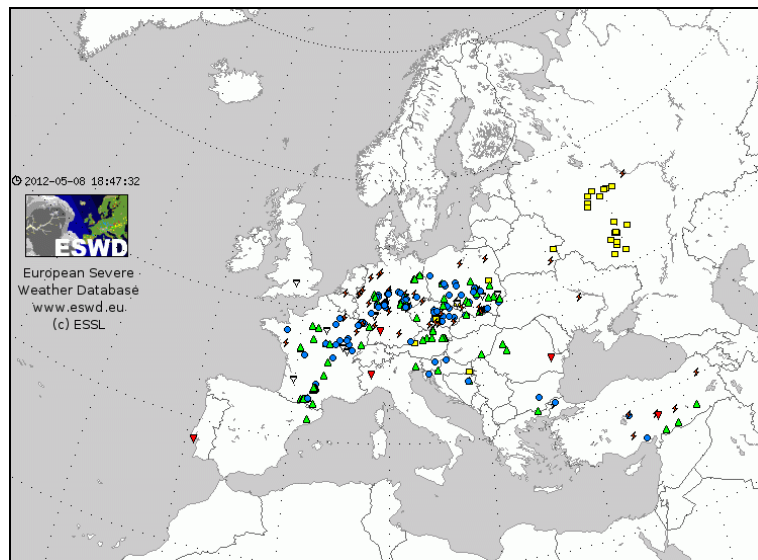


Figure: Example ESWD database display with several rain (blue), hail (green), tornado (red) and severe wind reports (yellow) plotted.

## Appendix 1: List of on-site participants

### **4 - 8 June**

Oscar van der Velde – Spain  
 Fernando Prates – U.K.  
 David Schultz – U.K.  
 Slawomir Guzek – Poland  
 Matheus Barczyk -- Poland  
 Grzegorz Mikutel – Poland  
 Matteo Buzzi – Switzerland  
 Eerik Saarikalle – Finland  
 Martin Ivanov – Bulgaria  
 Friedrich Föst – Germany  
 Marcus Boljahn – Germany  
 Joonas Eklund – Finland  
 Hannamari Jaakkola - Finland  
 Georg Pistotnik – ESSL  
 Alois Holzer – ESSL  
 Pieter Groenemeijer – ESSL

### **25 - 29 June**

Johannes Dahl – U.S.A.  
 Vesa Nietosvaara – Finland  
 Ivaylo Zamfirov – Bulgaria  
 Jozef Csaplár – Slovakia  
 Lucia Uhrinova – Slovakia  
 Andreas Asch – Switzerland  
 Johann Unegg – Austria  
 Tomas Pucik – Czech Republic  
 Erwin Hafenrichter – Germany  
 Guido-Peter Wolz – Germany  
 Wolfgang Schulz – Austria  
 Michael Butscheck – Austria  
 Aleksandra Arsic – Serbia  
 Vlado Spiridonov – Macedonia  
 Georg Pistotnik – ESSL  
 Alois Holzer – ESSL  
 Pieter Groenemeijer – ESSL

### **11 - 16 June**

Patrick Marsh – U.S.A.  
 Martin Setvák – Czech Republic  
 Kris Bedka – U.S.A.  
 Adam Michniewski – Poland  
 Lukasz Harasimowicz – Poland  
 Bernhard Forstner – Austria  
 Maja Rabrenovic – Serbia  
 Ieva Nariunaite – Lithuania  
 Inga Stankunaite – Lithuania  
 Ronald Prodingner – Austria  
 Thomas Krennert – Austria  
 Monika Weis – Austria  
 Jürgen Püschel –Germany  
 Georg Pistotnik – ESSL  
 Alois Holzer – ESSL  
 Pieter Groenemeijer – ESSL

### **2 - 6 July**

Hans Volkert – Germany  
 Johannes Dahl – U.S.A.  
 Ivan Tsonevsky – U.K.  
 Rafal Lokumski – Poland  
 Martin Leeson – U.K.  
 Rob Groenland – Netherlands  
 Michal Ogradnik – Poland  
 Paulo Pinto – Portugal  
 Andreas Schmölz – Austria  
 Thomas Knabl – Austria  
 Helge Tuschy – Germany  
 Karim Hamid – Belgium  
 Angel Marcev – Montenegro  
 Mehmet Yildirim - Turkey  
 Georg Pistotnik - ESSL  
 Alois Holzer - ESSL  
 Pieter Groenemeijer - ESSL

### **18 - 22 June**

Jim LaDue – U.S.A  
 Christoph Gatzen – Germany  
 Katarzyna Bednarek – Poland  
 Jan Deepen – Germany  
 Stefan Barthel – Germany  
 Laura Krumina – Latvia  
 Lionel Peyraud – Switzerland  
 Wolfgang Pöttschacher – Austria  
 Marcus Beyer – Germany  
 Marcus Paulat – Germany  
 Jure Cedilnik – Slovenia  
 Georg Pistotnik – ESSL  
 Alois Holzer – ESSL  
 Pieter Groenemeijer – ESSL

## Appendix 2: Expert Lectures

Expert lectures are daily returning lectures (60 minutes including question time) on a specific topic, starting after the Daily Briefing at 11:00 l.t. /0900 UTC has ended, i.e. around 11:30 l.t./0930. They are intended both for the audience on site and for remote participants that can follow the presentation through Centra teleconferencing software.

|           |        |                              |  |
|-----------|--------|------------------------------|--|
| Monday    | 4 June | Kris Bedka (SSAI@NASA)       | OT &Enh-V/ring-detections, Cloud-top Cooling |
| Tuesday   | 5 June | Fernando Prates (ECMWF)      | Extreme Forecast Index                       |
| Wednesday | 6 June | Oscar van der Velde          | Ingredients-based forecasting                |
| Thursday  | 7 June | David Schulz (U. Manchester) | Scientific Forecasting                       |
| Friday    | 8 June | David Schulz (U. Manchester) | Fronts and severe weather                    |

|           |         |                                |   |
|-----------|---------|--------------------------------|---|
| Monday    | 11 June | Caroline Forster (DLR; remote) | Cb-TRAM and Rad-TRAM                          |
| Tuesday   | 12 June | Patrick Marsh (NOAA)           | Heavy Precip. Fcst.: Patterns and Ingredients |
| Wednesday | 13 June | Martin Setvák (CHMI)           | Satellite sandwich image products             |
| Thursday  | 14 June | Paul James (DWD)               | NowcastMIX                                    |
| Friday    | 15 June | Patrick Marsh (NOAA)           | Ingredients-based tornado forecasting         |

|           |         |                            |  |
|-----------|---------|----------------------------|--|
| Monday    | 18 June | Kris Bedka (SSAI@NASA)     | OT &Enh-V/ring-detections, Cloud-top Cooling |
| Tuesday   | 19 June | Jim LaDue (NOAA)           | Convective Initiation                        |
| Wednesday | 20 June | Christoph Gatzen (ESTOFEX) | Derechoes in Europe                          |
| Thursday  | 21 June | Jim LaDue (NOAA)           | Storm modes                                  |
| Friday    | 22 June | Georg Pistotnik (ESSL)     | Convection and Orography                     |

|           |         |                               |  |
|-----------|---------|-------------------------------|--|
| Monday    | 25 June | Caroline Forster (DLR;remote) | Cb-TRAM and Rad-TRAM                         |
| Tuesday   | 26 June | Johannes Dahl (NCSU)          | Supercell dynamics                           |
| Wednesday | 27 June | Patrick Marsh (NOAA)          | Mesoscale Convective Systems                 |
| Thursday  | 28 June | Wolfgang Schulz (EUCLID)      | EUCLID: Mode of operation and performance    |
| Friday    | 29 June | Kris Bedka (SSAI@NASA)        | OT &Enh-V/ring-detections, Cloud-top Cooling |

|           |        |                              |  |
|-----------|--------|------------------------------|--|
| Monday    | 2 July | Ivan Tsonevsky (ECMWF)       | Extreme Forecast Index                 |
| Tuesday   | 3 July | Johannes Dahl (NCSU)         | Tornadogenesis                         |
| Wednesday | 4 July | Helge Tuschy (DWD)           | Hodographs and flash flood forecasting |
| Thursday  | 5 July | Hannamari Jaakkola (Vaisala) | Vaisala lightning detection technology |
| Friday    | 6 July | Hans Volkert (DLR)           | Field experiments                      |

## Appendix 3: References

Bedka, K. M., J. Brunner, R. Dworak, W. Feltz, J. Otkin, and T. Greenwald, 2010: Objective satellite-based overshooting top detection using infrared window channel brightness temperature gradients. *J. Appl. Meteor. And Climatol.*, 49, 181-202.

Bedka, K. M., J. Brunner, and W. Feltz, 2011: Objective overshooting top and enhanced-V signature detection for the GOES-R Advanced Baseline Imager: Algorithm Theoretical Basis Document.

Brunner, J.C., S.A. Ackerman, A.S. Bachmeier, and R.M. Rabin, 2007: A quantitative analysis of the enhanced-V feature in relation to severe weather. *Wea. Forecasting*, 22, 853–872.

Dotzek, N., P. Groenemeijer, B. Feuerstein, and A. M. Holzer, 2009: Overview of ESSL's severe convective storms research using the European Severe Weather Database ESWD. *Atmos. Res.* 93, 575-586.

Dworak, R., K. M. Bedka, J. Brunner, and W. Feltz, 2012: Comparison between GOES-12 overshooting top detections, WSR-88D radar reflectivity, and severe storm reports. *Wea. Forecasting*. In Press. (Download at: [http://angler.larc.nasa.gov/site/people/data/kbedka/Dworaketal\\_OT\\_NEXRAD\\_SevereWx\\_WeaForecasting2012.doc](http://angler.larc.nasa.gov/site/people/data/kbedka/Dworaketal_OT_NEXRAD_SevereWx_WeaForecasting2012.doc))

Groenemeijer et al., 2004: ESWD - A standardized, flexible data format for severe weather reports. European Conference on Severe Storms, León, Spain, 9-12 November 2004, 2 pp.

Groenemeijer et al., 2009: New capabilities of the European Severe Weather Database (ESWD). 5th European Conf. on Severe Storms, Landshut, Germany, 12-16 October 2009, 2 pp.

Hartung, D, J. M. Sieglaff, L. M. Counce, W. F. Feltz, 2012: An Inter-Comparison of UWCI-CTC Algorithm Cloud-Top Cooling Rates with WSR-88D Radar Data. Submitted to *J. Appl. Meteor. And Climatol.*

Kober, K. and A. Tafferner, 2009: Tracking and nowcasting of convective cells using remote sensing data from radar and satellite. *Meteorologische Zeitschrift*, Vol. 1, No. 18, 075-084.

McCann, D.W., 1983. The enhanced-V: a satellite observable severe storm signature. *Mon. Weather Rev.* 111, 887–894.

Setvak, M., D. T. Lindsey, P. Novak, P. K. Wang, M. Radova, J. Kerkmann, L. Grasso, S. Su, R. M. Rabin, J. Stastka, and Z. Charvat, 2010: Satellite-observed cold-ring-shaped features atop deep convective clouds. *Atmos. Res.*, 97, 80-96.

Sieglaff, J. M., L. M. Counce, W. F. Feltz, K. M. Bedka, M. J. Pavolonis, and A. K. Heidinger, 2011: Nowcasting convective storm initiation using satellite-based box-averaged cloud-top cooling and cloud-type trends. *J. Appl. Meteor. Climatol.*, 50, 110-126.

Wicker, L., Kain, J., Weiss, S., and Bright, D., 2005: A Brief Description of the Supercell Detection Index, available at: <http://spc.noaa.gov/exper/Spring 2005/SDI-docs.pdf>

Zinner, T., H. Mannstein, A. Tafferner, Cb-TRAM: Tracking and monitoring severe convection from onset over rapid development to mature phase using multi-channel Meteosat-8 SEVIRI data, Meteorol Atmos Phys, DOI 10.1007/s00703-008-0290-y, 2008.

Zinner, T., and H. D. Betz, 2009: Validation of Meteosat storm detection and nowcasting based on lightning network data. Proc. 2009 EUMETSAT Meteorological Satellite Conference, Bath, United Kingdom, 21 - 25 September 2009

Zrnic, D.S., D.W. Burgess and L.D. Hennington, 1985: Automatic Detection of Mesocyclonic Shear with Doppler Radar, J. Atmos. Oceanic Technol., 2, 425–438, 1985.